IOP Conf. Series: Journal of Physics: Conf. Series **882** (2017) 012009 doi:10.1088/1742-6596/882/1/012009

Quantitative visualization of oil-water mixture behind sudden expansion by high speed camera

Parham Babakhani Dehkordi, Luigi P.M Colombo, Manfredo Guilizzoni, Giorgio Sotgia, Fabio Cozzi

Politecnico di Milano, Department of Energy, via Lambruschini 4, 20156 Milan, Italy

Parham.babakhani@polimi.it

Abstract: The present work describes the application of an image processing technique to study the two phase flow of high viscous oil and water through a sudden expansion. Six different operating conditions were considered, depending on input volume fraction of phases, and all of them are resulting in a flow pattern of the type oil dispersion in continuous water flow. The objective is to use an optical diagnostic method, with a high speed camera, to give detailed information about the flow field and spatial distribution, such as instantaneous velocity and in situ phase fraction. Artificial tracer particles were not used due to the fact that oil drops can be easily distinguished from the continuous water phase and thus they can act as natural tracers. The pipe has a total length of 11 meters and the abrupt sudden expansion is placed at a distance equal to 6 meters from the inlet section, to ensure that the flow is fully developed when it reaches the singularity. Upstream and downstream pipes have 30 mm and 50 mm i.d., respectively. Velocity profiles, holdup and drop size distribution after the sudden expansion were analyzed and compared with literature models and results.

1. Introduction and literature

This work presents some preliminary results of an experimental investigation about the in situ oil volume fraction (holdup), velocity profiles and drop size distribution for two phase oil-water flow behind abrupt expansion in a horizontal pipe, by means of a visualization technique.

Laser-based techniques such as Particle Tracking Velocimetry (PIV) are widely used to characterize the hydrodynamic behavior of multiphase flow, feeding the continuous phase with small tracer particles which follow the main flow. A laser is used to illuminate the tracer particles in cross-section of pipe, while a digital camera is capable of capturing images frame by frame separated by short time delay. In PIV the frame acquisition is synchronized with the laser pulses, and each frame is subdivided into small interrogation window size. Each interrogation area in an image is linked to the corresponding interrogation area in the following frame. The second interrogation window must be sufficiently large to include all particles contained in the first interrogation window; on the other hand, care must be taken to properly select the second interrogation areas because, enlarging interrogation window would considerably reduce pixel resolution in the first window and increase computation time, as emphasized by Keane and Adrian [1]. After filtering and thresholding, pixel areas representing dispersed phase particles

can be identified. The particles would move and shift from one image to another. Hence, the cross-correlation function is able to statistically measure the level of match between two frames. The result of above procedure is a correlation plane, whose highest value can be used as a direct appraisal of the particle image displacement. The velocity of particles is then estimated by dividing the measured displacement and the time delay between consecutive frames. In the past decades, many researchers used PIV to characterize two-phase flow, mainly gas-liquid, in different pipe configurations. Delnoij [2] developed a new ensemble correlation PIV technique for a bubble column (so in bubbly flow regime), where movement of both the liquid phase (water) and the bubbles is recorded by a single CCD camera and using bubble-tracer patterns. The instantaneous velocity field and bubble concentration were detected using cross-correlation technique. The flow regime under investigation was bubbly flow. Polystyrene particles with sauter mean diameter of 250 μm, a density of 1070 $kg \cdot m^{-3}$ were used as tracer particle. The results showed that velocity difference between water and air must be sufficiently large to avoid overlap between the two displacement correlation peaks. Zhou et al. [3] used PIV to perform liquid phase turbulence measurement of liquid phase in an air-water two phase flow in a 50 mm i.d. horizontal pipe using PIV. Moreover, an optical phase separation approach/planar laser-induced fluorescent (PLIF) method was also used to differentiate bubbles from tracer particles in domain, and the local void fraction was measured using a four sensor conductivity probes. They compared the results from PIV measurements with literature ones using thermal anemometry for the same condition. Then, superficial liquid velocity was computed from local velocity and void fraction measurements. Difference in superficial liquid velocity between PIV and hot film anemometry (HFA) was found to be ±7% for void fraction less than 20%. Application of the PIV technique for two-phase gas-liquid for different configurations can be found also in Hassan et al. [4] and Gui et al. [5].

Although many works have been accomplished about gas-liquid flow, a few studies can be found regarding the application of particle velocimetry to liquid-liquid two phase flow. Augier et al. [6] performed tests about a dense liquid-liquid homogeneous flow based on PIV, considering a refractive index matching technique, in a vertical column. The objective was to measure local velocity field and phase fraction. The liquid-liquid system was composed of n-Heptane (dispersed), with viscosity of 4.5×10^{-4} $Pa \cdot s$ and density 683.7 $kg \cdot m^{-3}$, as well as mixture of 50% Glycerol-water solution as continuous phase. Sintered glass particles with diameter of 10 μm were selected as tracer particles because they have hydrophilic features, thus they would not penetrate to the organic dispersed phase. The laser sheet with 0.2×10^{-3} m thickness is responsible for illuminating the flow generated by a 20 mJ double pulsed Nd:Yag laser. The frequency of laser is ranged from 1 to 15 Hz with wavelength of 532 nm. The time delay between two flashes was between 5 and 10^4 μs, and a CCD camera with a 1008×1018 pixels resolution was used to record the flow. A sophisticated post processing was carried out, considering a 64×64 pixels interrogation area. The oil phase fraction was varied between 0 and 0.4 and local drag coefficients were measured from tests. The comparison of local drag coefficients (as a function of phase fraction) and models in literature was made, showing that classical drag coefficient laws underestimated the influence of phase fraction on drag coefficient.

The work by Pulvirenti and Sotgia [7] may also be cited, considering the application of PIV to stratified wavy oil-water flow. Mineral oil (μ_o=0.95 $Pa \cdot s$ and ρ_o=890 $kg \cdot m^{-3}$) and tap water were used as test fluids. The experimental tests were conducted in a horizontal 40 mm i.d. pipe to investigate the wavy structure of stratified flow. A mixture velocity of 0.7 $m \cdot s^{-1}$, and input water volume fraction of 0.37 were considered for analysis. Silver coated hollow glass spheres were selected as particle tracer for seeding water. Instantaneous water velocity fields were detected using 2D PIV technique and water velocity maps developed. Furthermore, the position of the oil-water interface was detected and circulation of water in the region between each couple of consecutive crests of oil core waves was recognized.

Morgan et al. [8] performed experimental tests about liquid-liquid flow in a horizontal circular tube. An aliphatic hydrocarbon oil (Exxsol D80, μ_o=2.3×10-3 $Pa \cdot s$ and ρ_o=796 $kg \cdot m^{-3}$) and glycerol-water solution ($\mu_{w-g}=47 \times 10^{-3}$ $Pa \cdot s$ and ρ_{w-g}=1,205 $kg \cdot m^{-3}$) were used as test fluids. The concentration of glycerol must be regulated in order to match refractive index between oil and glycerol-water mixture (RI=1.44), the authors also emphasized the importance of refractive index between fluids and pipe wall. Hence, a

proper choice of pipe wall materials is crucially important for image processing technique. In their work, light distortion due to curvature of pipe cross-section was corrected by using a graticule technique. They focused on the flow regime transition from stratified to dual continuous flow, used high speed PLIF, PIV, and Particle Tracking Velocimetry (PTV). They realized that the mixture of glycerol-water solution (heavier and more viscous phase) moved in laminar, while Exxsol oil was in a turbulent flow.

As evident from the cited literature, PIV characterization of liquid-liquid flow in straight pipe has been thoroughly performed. On the contrary, information regarding oil-water flow through singularities is still lacking. Concerning flow of oil-water through abrupt change of pipe cross-section, the authors were able to find four contributions in literature, Hwang and Pal [9], Balakhrisna et al. [10], Kaushik et al. [11], and Colombo et al. [12], all of them unrelated to PIV or similar techniques. The present study is therefore aimed at extending the application of image processing techniques, with a high speed camera, to two-phase oil-water flows behind a sudden expansion, in order to quantitatively explore the effect of such singularity on the flow field and holdup. Instantaneous velocity fields for oil drops, in-situ volume fractions, and oil drop size distribution were determined and the results were compared to literature models and correlations.

2. Experimental setup

The oil-water facility is available at Multiphase Thermo-Fluid laboratory, Department of Energy, Polytecnico di Milano. The schematic of test facility is shown in Fig. 1. The test pipe, having a total length of 11 m, is made Plexiglass® to allow the visual inspection of flow, that was performed by a high speed camera. Oil and water injectors were originally designed to ensure the onset of a stable core-annular flow, with water touching the duct wall and an oil core. However, changing the input flow rate of the phases it is also possible to obtain a dispersed flow, (for further information see e.g. Sotgia et al. [13]). For the present experimental campaign, the test section includes a sudden expansion at a distance of 7 m from the inlet mixing section, with upstream and downstream internal pipe diameters of 30 mm and 50 mm, respectively. A total of 12 pressure taps are mounted, almost uniformly distributed along the pipe, and a pressure transducer (Setra® model 230, full scale: 1 psi=6895 Pa) is installed to measure the pressure drop. The rheological properties of oil and water are reported in Tab. 1. Oil and water interfacial energy was measured at the Chemistry, Material, and Chemical Engineering Department, Politecnico di Milano, by means of a LAUDA tensiometer, while the oil viscosity by the laboratory "INNOVHUB-Stazioni Sperimentali per l'Industria- Divisione Stazione Sperimentale per le Industrie degli Oli e Grassi (SSOG)" and its temperature dependence may be expressed as:

$$\mu_o = 3.44 \exp(-0.71\ T) \qquad (1)$$

Table 1. Rheological properties of mineral oil and tap water for experimental tests

Rheological properties at $20\,^{\circ}C$	Tap water	Mineral oil
ρ [kg·m^{-3}]	998	910
μ [Pa·s]	1.026×10^{-3}	0.838
$\sigma_{o\text{-}w}$ [J·m^{-2}]	0.02	

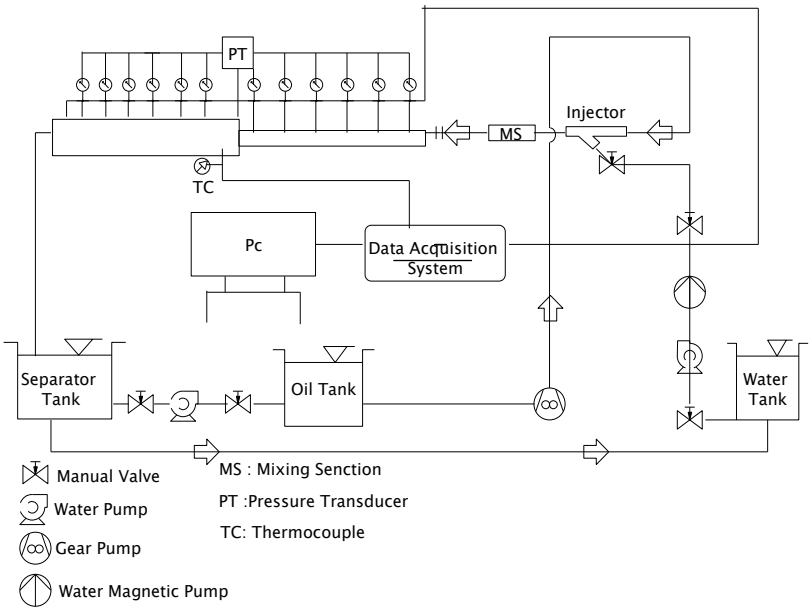

Figure 1. Schematic of the test facility

The water flow rate was measured by a magnetic flow meter (accuracy ±0.5% of reading), while the oil volume flow rate was measured by a calibrated gear metering pump. Figure 2 shows the data acquisition system, including the high speed camera, and the test section, within which the mixture is flowing from right to left. A white sheet was placed at the back of pipe section to avoid disturbances in the pictures from the back wall. The high speed camera was placed perpendicular to the pipe section and at the same height, while two lamps (halogen, 800 W each) were used to provide the necessary illumination. As a side view and not a cross-section of the duct is acquired, what is in fact obtained is a 2D projection of the flow, including perspective effect and optical distortions due to the different refraction indices of water, Plexiglass® and air. Consequently, there is no way to identify coplanar drops and to discriminate three-dimensional components of the drop velocity. As this is preliminary analysis, these issues were not taken into account. For this study, tracer particles were not used for seeding as done for PIV application because objective of the work is to measure velocity profile of oil drops, which can be easily distinguished from water continuous phase. Tracer particles are usually used to characterize the flow of continuous phase. Furthermore, the use of tracer particles to measure also velocity of continuous phase requires two cameras, one for dispersed oil drops and another for tracer particles. Post-processing of the acquired images was done using Dantec Dynamic Studio v3.12 [14] software. Table 2 reports the camera settings for the experimental tests.

Table 2. Camera setting for experimental tests

Pixel resolution [pixels]	1024×400
Time delay between frames [μs]	1666.50
Frame rate [fps]	600
Field of view [m^2]	0.37×0.05
Interrogation window[pixels]	64×64

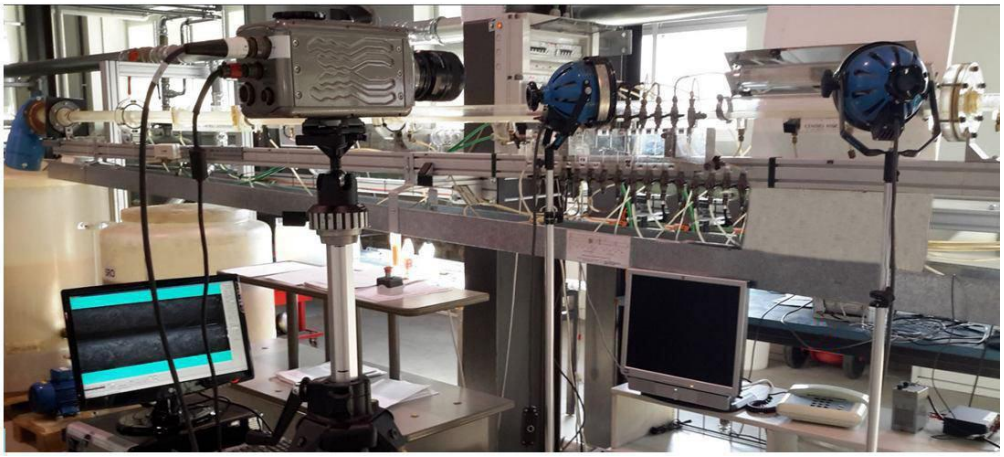

Figure 2. Data acquisition system and test section

3. Governing parameters and experimental conditions

In the following section, the most important governing parameters for oil-water mixtures will be summarized. The superficial velocity or volumetric flux J (ms^{-1}) is defined as the ratio between the volumetric flow rate of each phased and the cross-sectional area of the pipe. The sum of the two superficial velocities of the phases is the total mixture velocity:

$$J_{o-w} = J_o + J_w \tag{2}$$

The oil volume fraction, ε_o is defined as the ratio between superficial velocity of oil and the superficial velocity of the mixture:

$$\varepsilon_o = \frac{J_o}{J_{o-w}} \tag{3}$$

The water volume fraction can be defined in a completely analogous way, or simply obtained by $\varepsilon_w = 1 - \varepsilon_o$. The phase holdup is calculated by dividing the superficial velocity of each phase and the actual (effective) velocity as:

$$H_o = \frac{J_o}{U_o} \quad , \quad H_w = \frac{J_w}{U_w} \tag{4}$$

The slip ratio is the ratio between the effective oil velocity and the effective water velocity:

$$S = \frac{U_o}{U_w} \tag{5}$$

Obviously, the phase volume fraction is in general different from the phase holdup and the slip ratio is different from 1; they both depend on flow regime under investigation. For dispersed flows where the dispersed phase moves at the same velocity of the continuous carrier phase, the phase volume fraction and the holdup becomes equal and the slip ratio becomes unitary (“homogeneous flow”). The investigated experimental conditions are tabulated in Tab. 3 (with superficial velocities evaluated downstream of singularity, thus in the larger pipe).

Table 3. Summary of experimental test conditions

Case test	J_o [m·s^{-1}]	J_w [m·s^{-1}]	ε_o [-]	Re_{os} [-]	Re_{ws} [-]
1	0.29	0.70	0.29	16	35,297
2	0.29	0.84	0.25	16	42,356
3	0.44	0.70	0.38	24	35,297
4	0.44	0.56	0.46	24	28,237
5	0.59	0.70	0.45	32	35,297
6	0.59	0.84	0.41	32	42,356

Values of Reynolds number for Phases (Re_{os} and Re_{ws}) are calculated with the superficial velocities. In terms of flow pattern, all the conditions under investigations are related to the dispersion of oil drops in water.

4. Result and Discussion

Measurements were performed in the region behind the sudden expansion to evaluate the effect of the latter on in-situ velocity profiles, holdup and drop size distribution, in the flow re-development region region. Figure 3 shows a typical example of dispersed flow of oil drops in water continuous flow for J_o=0.29 m·s^{-1} and J_w=0.84 m·s^{-1}. Two frames, A and B, are required to create a correlation plane. The images A and B are recorded at time instant t and t+Δt, respectively, with Δt=1666.5 μs. It is worth noting that larger values of the time interval cause as higher probability for oil particles to leave the light plane. The images are converted in grey scale (Fig. 3-b) and then they must be binarized by a threshold technique to distinguish between oil drop particles and water continuous flow, see Fig 3-c. The particle shift between image A and B allows measuring the local velocity profile over the entire domain, from which spatially-averaged values can be determined (within the already cited limits related to the use of side views). This can be done over horizontal lines, to get vertical (so radial for the duct) velocity profiles, or over the whole domain. The calculations are then repeated over a large number of image couples, to obtain statistically significant values of the time-average of such velocities. As an example, Fig. 4 shows the evolution of the time-averaged velocity of the oil particles over the whole domain as a function of number of image couples used for the calculation, for test case 2.

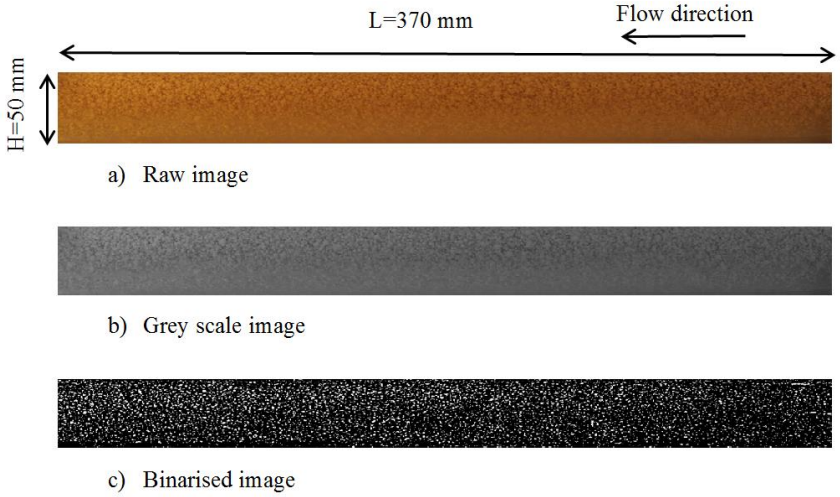

Figure 3. Typical example of high viscous-oil dispersion in water continuous flow: a) raw image, b) grey-scale image, c) binarized image

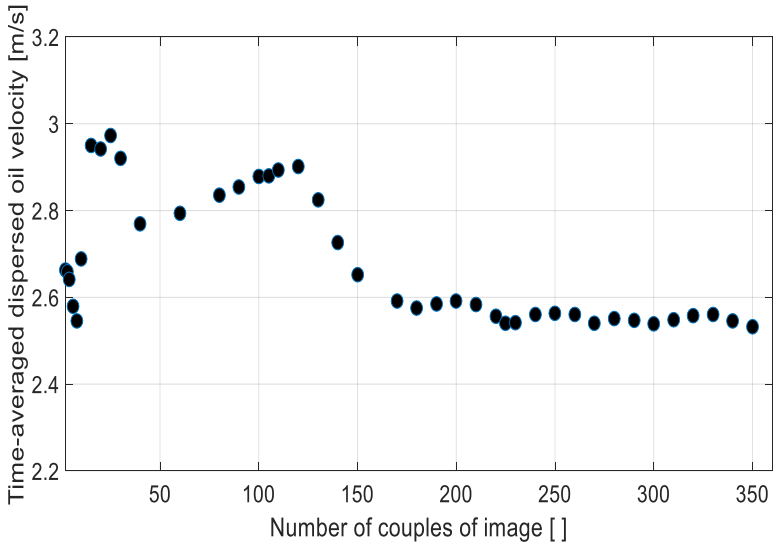

Figure 4. Cross-sectional time-averaged oil particle velocity over the whole investigated domain as a function of the number of the used image couples for J_o=0.29 $m \cdot s^{-1}$ and J_w=0.84 $m \cdot s^{-1}$

As it is evident, the average begins to stabilize after 150 images. Therefore, in the current study, a total of 400 frames are used to analyze in-situ oil particle velocity and holdup. The measurement tests were acquired at 4 axial positions downstream the sudden expansion: L/D=1, 2.5, 4, 5.5. Each side view covers a horizontal length of 370 mm and in vertical the full duct diameter of 50 mm.

4.1 Velocity profiles

Figure 5 illustrates the velocity profile for the six cases reported in Tab. 1. For each test, the in-situ time-averaged velocity of oil particles is normalized by the mixture superficial velocity. It is evident from Fig.5 that the velocity profile has a 'top-hat' shape for the farthest axial positions from sudden expansion, while it has a Gaussian-like shape very close to the singularity. The flat velocity profile for positions far from singularity would seem to show that the oil-water flow is becoming fully developed. This seems also consistent with the fact that velocity distributions for cases 3-6 at axial distances of L/D=4 and L/D=5.5 are perfectly matched. Nevertheless, for lower input oil fraction the difference between the profiles at L/D=4 and L/D=5.5 gives an opposite indication of still undergoing development. For velocity profiles at axial distance of L/D=5.5, it can also be observed that the time-averaged velocity of oil particles becomes zero at bottom part of pipe cross-section. Two possible explanation of this result may be given. One is that after the abrupt change of cross section, the mixture velocity is lower than in the upstream pipe, and dispersed oil drops tend to migrate to the upper part of tube. The second is related to the fouling of the internal surface of the pipe, as Plexiglass® is an oleophilic material. The analysis of the velocity profiles at the axial distance L/D=1 shows that time-averaged velocity of oil particles is much higher at the centerline than in the regions very close to the pipe wall, as it can be reasonable given the fact that the mixture has just entered the larger downstream pipe, so the central part behaves partially as a "jet". The results of measurements from image processing reported in Fig. 5 proved that development length after this kind of singularity for high viscous oil-water is dependent on the oil input volume fraction. For higher values of oil volume fraction, the flow becomes fully developed at axial distance of L/D=4.

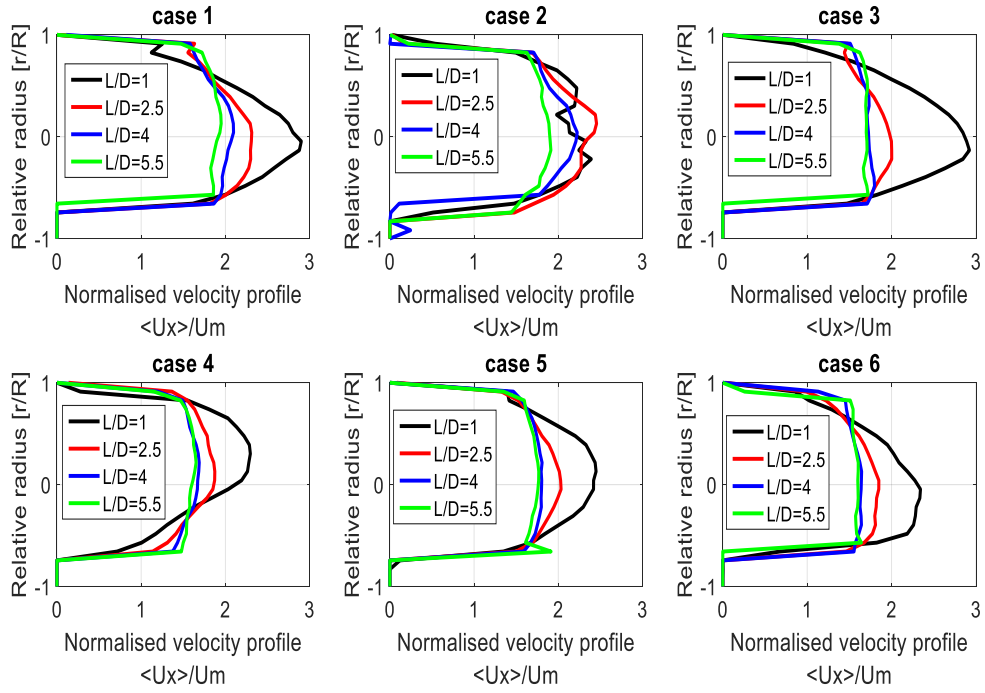

Figure 5. Time-averaged velocity profile at different axial position of L/D=1, L/D=2.5, L/D=4 and L/D=5.5 for the six cases reported in Table 1

4.2 Time-averaged oil holdup

To calculate the cross-sectional average of the oil holdup, it is necessary to calculate the cross-sectional average velocity profile for each operating condition as:

$$< U_o >= \frac{1}{A} \int u_o dA \qquad (6)$$

The time-averaged velocity in domain is automatically extracted by Dantec's Dynamic Studio 3.12 software. Thus, in each point in radial direction, time-average velocity is obtained. The oil holdup can be estimated as the ratio between the oil superficial velocity and the cross-sectional average velocity:

$$< H_o >= \frac{J_o}{<U_o>} \qquad (7)$$

The time-averaged cross-sectional water holdup can be simply calculated as; $<H_w>=1-< H_o >$.

Arney et al. [15] developed an empirical correlation based experimental data using quick closing valve for core-annular regime:

$$H_o = 1 - \varepsilon_w[1+0.35(1 - \varepsilon_w)] \qquad (8)$$

Colombo et al. [12] measured liquid holdup by quick closing valve method over some hundreds experimental points for oil-water flows in pipes having constant diameter and including two different sudden contractions, from 50 mm to 40 mm i.d. (contraction ratio, ζ=0.64) and from 50 mm to 30 mm i.d. (ζ=0.36). Oil was the same than in the current study, while the flow regime under investigation were both dispersion of oil in water and core-annular flow. The experimental results about oil holdup were compared to Arney correlation, showing a very good agreement (average absolute error 5.15%, and 5.88% for ζ=0.64 and ζ=0.36, respectively). This proved that Arney correlation works well for dispersed flow regime. Thus, comparison of cross-sectional time-average oil holdup estimated by image processing technique to Arney correlation was performed in this study. Figure 6-a shows oil holdup versus input volume fraction for the axial distance L/D=5.5, which should be the one less influenced by sudden expansion. All data falls below bisector, showing that the oil-water mixture cannot be treated as a homogeneous flow, even if it is an oil dispersion in water. Furthermore, as the oil holdup is lower than the oil input volume fraction, the oil velocity is higher than the water velocity and the oil-to-water slip ratio is always significantly larger than unity, as it will be further discussed in the following. These findings may appear surprising for a dispersed flow regime, that is often modeled as if mixture behaved homogeneously; but it must be considered that it is evident from visual inspection that all the oil particles move to the upper part of tube due to presence of the larger pipe downstream of the singularity, thus the distribution of oil particles becomes inhomogeneous.

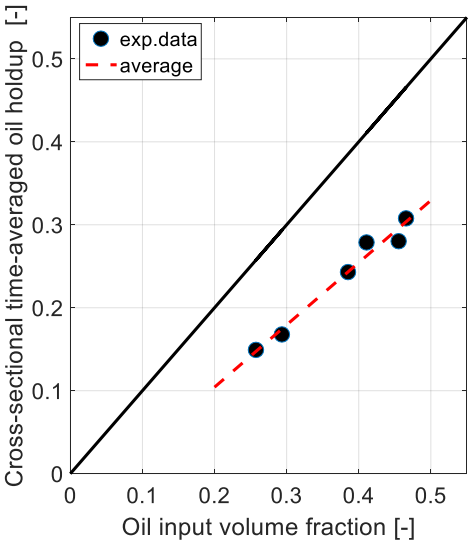

Figure 6. a) cross-sectional time-averaged oil holdup against oil input volume fraction

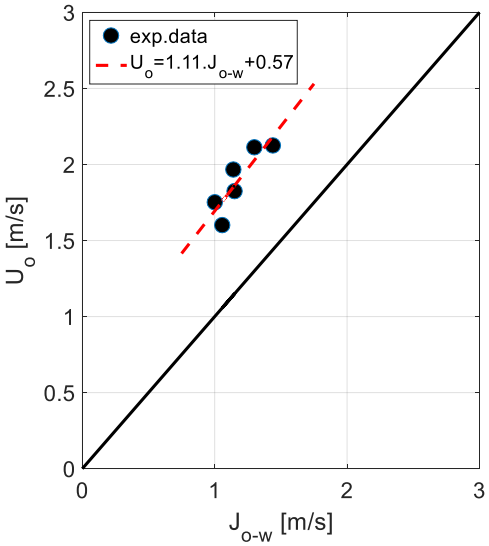

Figure 6. b) cross-sectional time-averaged oil velocity against mixture superficial velocity

The fact that oil is moving faster is consistent with the results obtained by Morgan et al. [8] and Colombo et al. [12]: the quantitative values on the contrary are different from the results for uniform-diameter pipes and sudden contractions, very likely due to the significant effect of the expansion in the first diameters of the downstream pipe. The results of oil holdup in Fig 6-a are consistent with the work of Colombo et al. [12] and Morgan et al. [8].

Brauner [16] emphasized that for low mixture superficial velocity where water is the continuous phase (conditions that applies to the present study), relatively large oil drops can be formed which considerably affect slippage between oil and water continuous phase. She suggested the use of Zuber-Findlay [17] drift flux model to characterize two phase oil-water dispersion flow. In the framework of the drift-flux model, the oil velocity can be modeled as:

$$U_o = C_o J_{o-w} + u_d \qquad (9)$$

where C_o is a distribution parameter, which is in relation to the phase velocities and distribution within the duct, while u_d is the drift velocity. Figure 6-b shows average oil drop velocity as a function of mixture superficial velocity, where linear fitting of experimental data by image processing evidences that $C_o>1$, meaning that drop concentration is higher at the center of pipe, as supported by the work of Colombo et al. [12] and Brauner [16]. The amount of available data from the present campaign is regrettably too limited for a really significant validation of the Zuber-Findlay drift flux model after singularity, and this can be topic for further investigation. Figure 7-a. reports the values of the slip ratio between oil particles and water, defined by Eq. 5, as a function of the oil input volume fraction. The homogeneous flow model is represented by the solid line at s=1. The results are consistent with those about holdup, evidencing how the homogeneous model largely under-predict the measurements from image processing. This under-prediction is not varying significantly with the oil input volume fraction, it just oscillates in a range between 1.75 and 2.25. These results are contrary to what Morgan et al. [8] observed for low viscosity oil-water flow in straight pipe, where slip ratio under-prediction increases at

increasing oil input volume fraction. Finally, the results of comparison between oil holdup estimated using Arney correlation and oil holdup by image processing are reported in Fig. 7-b. Data align themselves around the +25% line with respect to the predictions of the correlation, in contrast with the very good agreement found for uniform-diameter pipes and contractions (Colombo et al. [12]). This is a further evidence that the influence of the sudden expansion at L/D=5.5 is still considerable, even if the velocity profile appears fully developed.

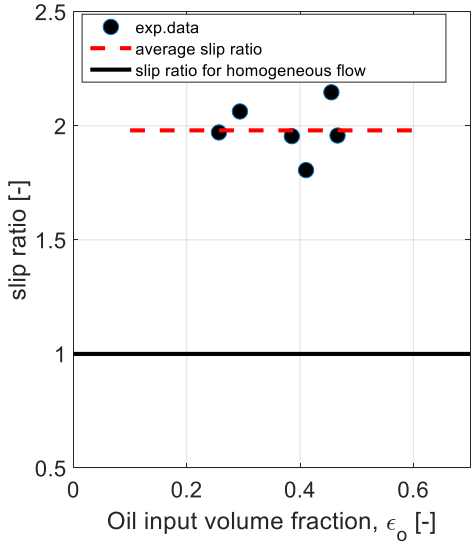

Figure 7. a) slip ratio versus oil input volume fraction

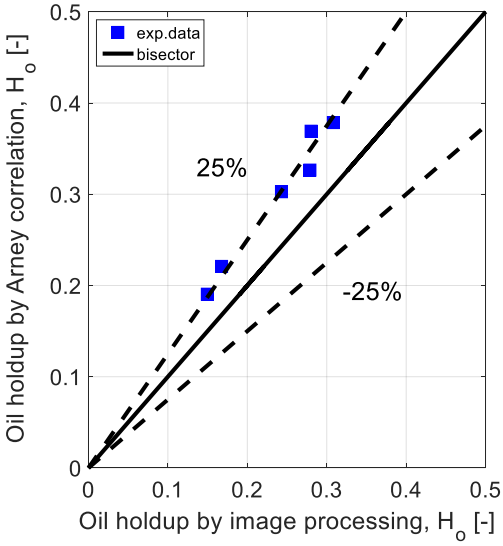

Figure 7. b) measured oil holdup by image processing against oil holdup predicted by Arney correlation [15]

4.3 Drop size distribution

The identification of oil drops in the processed images allowed also performing an analysis of the drop size distribution. After image binarization, white blobs corresponding to oil drops can be identified and their dimensions calculated. Once again neglecting optical distortions, and assuming a spherical shape for the drops, an effective drop diameter is calculated as:

$$d_{eff} = 2\sqrt{\frac{A_d}{\pi}} \qquad (10)$$

From which the average drop diameter can be then calculated:

$$\mu_d = \frac{1}{N}\sum_{i=1}^{N} d_{eff} \qquad (11)$$

A major problem in measuring drop size is that depending on the thresholding/filtering steps and on the parameters used during the image processing, blobs representing drops may merge. A a consequence, different threshold values result is different drop size distribution and much care must be taken to select a proper threshold value. Lower threshold values may result in loosing

drops, while increasing threshold values may cause fictitious merging of them. Automated selection of threshold values can prove unreliable, so direct visual comparison with the original images was used here to select suitable threshold values. Figure 8 shows a typical example of drop size distribution for case 2 (J_o=0.29 m·s^{-1}, J_w=0.84 m·s^{-1}), while for comparison Fig. 9 illustrates some instantaneous images from cases 1-4, evidencing how larger structures, more similar to "flakes", coexist with the population of oil drops. This reflects in the presence of large structures in the histogram, which in fact influence significantly the moments of the drop size distribution, despite their very limited numerical amount: the histogram is obviously right skewed (as negative values cannot be present), with mean at 1.60 mm and median at 0.93 (standard deviation 1.90 mm). Given the described issue, the median – which is less sensitive to extreme values than the mean is probably the most reliable indicator. The average drop size for this case is lower that what Morgan et al. [8] observed for low oil viscosity-water flow. Even if increasing viscosity of the dispersed phase (at the same superficial velocity) can postpone the process of drop deformation and breakup, and breakage is higher in regions near to pipe wall than in the center of pipe (see Lovick and Angeli [18]), it may be that the effect of the sudden expansion in breaking the oil particles (drops and flakes) overcomes the influence of oil viscosity.

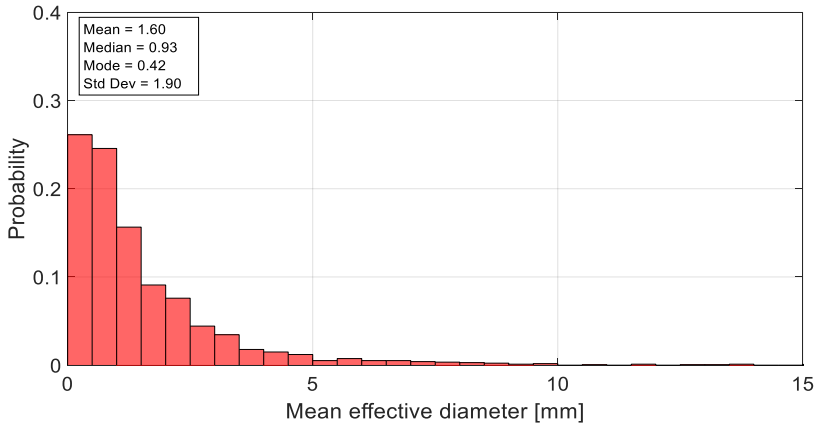

Figure 8. Drop size distribution histogram for case 2 (J_o=0.29 m·s^{-1}, J_w=0.84 m·s^{-1})

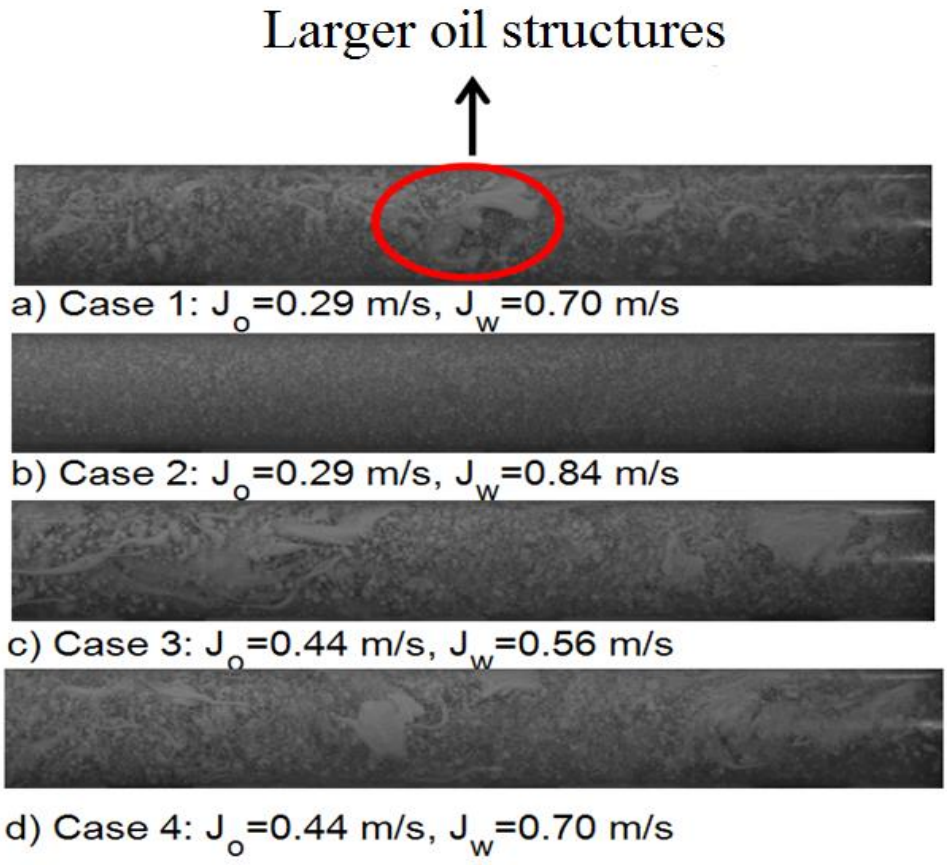

Figure 9. Flow visualization by high speed camera for cases 1-4

5. Conclusions

An oil dispersed in water continuous flow was experimentally investigated using a non-intrusive optical technique, in a 11 m long horizontal pipe with a sudden section expansion from 30 mm to 50 mm i.d. Very viscous oil and tap water were considered as test fluids. Instantaneous 2D velocity fields for oil drops were measured by a cross-correlation technique, and velocity profiles for six cases were obtained. Oil liquid holdup was then calculated, taking into account the cross-sectional time-averaged oil velocity. Based on this quantity, the cross-sectional time-averaged values of oil and water velocities, and the slip ratio between the two phases were also calculated. The results showed that the effect of the sudden expansion on the velocity profiles in the downstream pipe is significant for axial positions close the singularity, than they seem to re-develop with a “top-hat” shape. Concerning cross-sectional time-averaged oil holdup, the results show that the oil-water mixture cannot be considered as a homogeneous flow because oil always move faster than continuous water, even though flow regime under investigation is dispersed flow. This is also supported by the fact that the value of slip ratio is always higher than unity and practically independent from oil input volume fraction. The holdup and slip results, together with the results of a comparison with the drift-flux model, also evidence that despite the shape of the velocity profiles, the flow after 5 diameters from the expansion seems still not developed.

References

[1] Keane R D and Adrian R J 1992 Theory ofcross-correlation analysis of PIV images *Appl. Sci. Res.* **49** 191–215
[2] Delnoij E 1999 Fluid dynamics of gas-liquid bubble columns - A theoretical and experimental study, PhD thesis, University of Twente
[3] Zhou X and Doup B 2013 Measurements of liquid-phase turbulence in gas-liquid two-phase flows using particle image velocimetry *Meas. Sci. Technol.* **24** 125303
[4] Hassan Y A, Blanchat T K and Seeley Jr 1992 Simultaneous velocity measurements of both components of a two-phase flow using particle image velocimetry drop *Int. J. Multiphas. Flow* **18** 371–395
[5] Gui L, Lindken R and Merzkirch W 1997 Phase-separated PIV measurements of the flow around systems of bubbles rising in water Proceedings of the ASME (American Society of Mechanical Engineers) Fluids Engineering Summer Meeting, 97–3103
[6] Augier F, Masbernat O and Guiraud P 2003 Slip velocity and drag law in a liquid-liquid homogeneous dispersed flow *AIChE J* **49**(9) 2300–2316
[7] Pulvirenti B and Sotgia G 2004 Experimental analysis of water fluid dynamics in oil-water wavy-stratified regime, 3rd International Symposium on Two-Phase Flow Modelling and Experimentation, Pisa, Italy
[8] Morgan R G, Markides C N, Zadrazil I, Hewitt G F 2013 Characteristics of horizontal liquid-liquid flows in a circular pipe using simultaneous high-speed laser-induced fluorescence and particle vcelocimetry drop *Int. J. Multiphas. Flow* **49** 99–118
[9] Hwang C-Y J and Pal R 1997 Flow of two-phase oil/water mixtures through sudden expansions and contractions *Chem. Eng. J.* **68**(2-3) 157–163.
[10] Balakhrisna T G 2010 Oil-water flows through sudden contraction and expansion in a horizontal pipe – Phase distribution and pressure drop drop *Int. J. Multiphas. Flow* **36**(1) 13–24
[11] Kaushik V V R, Ghosh S, Das G and Das P K 2012 CFD simulation of core annular flow through sudden contraction and expansion *Petrol. Sci. Techol.* **86-87** 153–164
[12] Colombo L P M, Guilizzoni M, Sotgia G M and Marzorati D 2015 Influence of sudden contractions on in situ volume fractions for oil-water flows in horizontal pipes drop *Int. J. Multiphas. Flow* **53** 91–97
[13] Sotgia G, Tartarini P and Stalio E 2008 Experimental analysis of flow regimes and pressure drop reduction in oil-water drop *Int. J. Multiphas. Flow* **34**(12) 1161–1174
[14] Dantec dynamic studio user guide v3.12 2010
[15] Arney M S, Bai R, Guevara E, Joseph D D and Liu K 1993 Friction factor and holdup studies for lubricated pipelining – I. experiments and drop *Int. J. Multiphas. Flow* **19**(6) 1061–1076
[16] Brauner N 2001 The prediction of dispersed flows boundaries in liquid-liquid and gas-liquid systems drop *Int. J. Multiphas. Flow* **27**(5) 885–910
[17] Zuber N and Findlay J A 1965 Average volumetric concentration in two-phase flow systems *J. Heat Transf.* **87** 453–468.
[18] Lovick J and Angeli P 2004 Droplet size and velocity profiles in liquid-liquid horizontal flows *Chem. Eng. Sci.* **59** 3105–3115